Research Square

Preprints are preliminary reports that have not undergone peer review.
They should not be considered conclusive, used to inform clinical practice,
or referenced by the media as validated information.

Green synthesis of cerium oxide nanoparticles using Falcaria Vulgaris leaf extract and its anti-tumoral effects in prostate cancer

Danial Taherzadeh
Mashhad University of Medical Sciences
Hamed Amiri
Mashhad University of Medical Sciences
Safeih Ebrahimi
Mashhad University of Medical Sciences
Arash Ghafarpour
Abnoos Skin & Hair Clinic
Nazanin Samandarinejad
Abnoos Skin & Hair Clinic
Majid Darroudi
Mashhad University of Medical Sciences
Seyed Isaac Hashemy (hashemyi@mums.ac.ir)
Mashhad University of Medical Sciences

Research Article

Keywords: Cerium Oxide, Nanoparticle, Green Synthesis, Falcaria Vulgaris, Prostate Cancer

Posted Date: February 14th, 2023

DOI: https://doi.org/10.21203/rs.3.rs-2568195/v1

License: This work is licensed under a Creative Commons Attribution 4.0 International License.
Read Full License

Additional Declarations: No competing interests reported.

Abstract

Over recent years, metal oxide nanoparticles have been extensively investigated due to their potential biomedical applications. This study aimed to describe a simple and eco-friendly method for the green synthesis of cerium oxide nanoparticles (CeO_2 NPs) using *Falcaria vulgaris* (*F. vulgaris*) leaf extract as a capping agent and to evaluate their anti-cancer effects on human prostate cancer cells (PC3). The phyto-synthesized CeO_2 NPs were characterized by UV–visible spectroscopy, X-ray diffraction, transmission electron microscope, Fourier transform infrared spectroscopy, scanning electron microscope, and energy-dispersive X-ray spectroscopy. The UV-Visible spectrum showed a peak at 313 nm with a band gap energy of 3 eV. Microscopic results revealed that CeO_2 NPs mainly were spherical. In addition, the XRD pattern confirmed the crystalline structure of green synthesized CeO_2 NPs with an average crystalline size of around 19.5 nm. In biological experiments, the results of the resazurin assay indicated the significant cytotoxic activity of CeO_2 NPs against PC3 cells with an IC_{50} at 113.6 µg/ mL. The real-time PCR results revealed that CeO_2 NPs effectively regulate PC3 cell proliferation, apoptosis, and migration by modifying the expression of cell cycle-related proteins (c-Myc, cyclin D1, p21), and apoptosis-related genes (Bcl-2 and Bax), and migration-related genes (MMP-2 and MMP-9). Overall, these findings suggest that the green fabricated CeO_2 NPs from *F. Vulgaris* can be used as a novel therapeutic agent for prostate cancer treatment.

1. Introduction

Nanoparticles (NPs) are routinely defined as ultra-fine particles with diameters ranging from 1 to 100 nm that exhibit unique optical, magnetic, and electrical properties [1]. Presently, different metal and metal oxide nanoparticles are being produced and used in a wide variety of fields, including analytical chemistry [2], photocatalytic potential [3], nano-diagnostics [4], agriculture [5], solar cells [6], and environmental remediation [7]. Additionally, there has been a growing interest in using nanoparticles for different biomedical applications such as bioimaging, hyperthermia, targeted drug delivery, and cancer therapy, over the last few years [8]. Despite various applications, the use of metallic-based nanoparticles may have adverse impacts on human health. Due to their small size and large surface area coupled to other physicochemical characteristics such as charged surface and metal contaminants, nanoparticles may show unexpected genotoxic properties [9]. Nanoparticles can cause DNA damage directly or indirectly by inducing oxidative stress and inflammatory responses. Small nanoparticles may pass through cellular membranes and access the nucleus, where they can directly interact with DNA molecules, causing damage [10].

Various chemical and physical procedures have been exploited in the synthesis of nanoparticles. However, these methods suffer many limitations such as low yield, the use of hazardous chemicals, expensive reagents, lengthy reaction time, and high energy requirements [11]. Thus, there is a pressing need to develop biocompatible, safe, sustainable, efficient, and economical methods for the synthesis of nanoparticles. Recent studies have indicated that green synthesis approaches are simple, fast, energy-

efficient, clean, biocompatible, cost-effective, and environmentally friendly [12, 13]. Green synthesis methods offer the possibility to produce nanoparticles without the usage of harsh chemicals or the generation of toxic by-products for synthesis and the subsequent functionalization of nanoparticles. Therefore, green synthesized NPs can suitable for biomedical applications [14]. In green synthesis routes, different biological sources like yeast, fungus, bacteria, and plant constituents can be potentially used instead of chemical agents to produce nanoparticles [15]. Among various natural resources, plant biomaterials seem to be the best candidates for the large-scale biosynthesis of nanoparticles. Plant-mediated synthesis is also straightforward and does not require specific conditions needed in conventional physical/chemical methods. Furthermore, the nanoparticles produced using plants are more varied in size and shape in comparison with those produced by other bio-organisms [16]. Many bioactive constituents in plant extracts including flavonoids, glycosides, alkaloids, phenolic acids, terpenoids, amino acids, proteins, and enzymes, play a major role in the formation and stabilization of nanoparticles [17]. It is found that plant biomolecules are involved in the biological reduction of metal salts into metal NPs. These biomolecules also act as capping agents hence responsible for the stability of nanoparticles [18].

Physicochemical characteristics of biosynthesized nanoparticles such as size distribution, shape, chemical composition, surface charge, and surface chemistry play important roles in the pharmaceutical potentials, cellular interactions, and toxic manifestations of nanoparticles. In addition, various natural sources that act as bio-reducing and bio-capping agents in the green synthesis process may affect the biological activity of nanoparticles [19, 20]. The change in these factors can cause different cytotoxic responses [21]. For example, it was shown that the metallic nanoparticles of less than 25 nm in size had a more cytotoxicity effect than ones with size distributions between 25 and 50 nm against cancer cells. Furthermore, it has been reported that the cellular internalization of phytofabricated Au-NPs with rod morphology was less than spherical Au-NPs in cancer cells. Surface functionality is also an important factor that may affect the biological activity of NPs. Surface functionalization of NPs by conjugating with biomolecules like pharmaceutical agents, antibodies, and aptamers can provide a chance to build multifunctional NPs for different purposes involving diagnosis, targeted drug delivery systems, etc [22].

Falcaria vulgaris (*F. vulgaris*) is an important medicinal plant belonging to the family Apiaceae [23]. *F. vulgaris* is a biennial and highly branched plant. In traditional medicine, it is used to treat gastric and duodenal ulcers [24]. In addition, previous studies have indicated *F. vulgaris* has notable hepatoprotective, antihyperlipidemic, nephroprotective, anti-diabetic, antibacterial, antifungal, anti-inflammatory, anti-cancerous, and antioxidant activities [25]. Phytochemical studies have revealed the presence of phytosterol, vitamin C, carvacrol, spathulenol, starch, and proteins in this plant [23, 26].

Cerium is the most abundant rare earth metal with atomic number 58. Cerium ions can generally exist in two oxidation states (Ce^{3+} and Ce^{4+})s. Hence, cerium oxide has two different oxide forms in bulk material: CeO_2 (Ce^{4+}) and Ce_2O_3 (Ce^{3+}) [27]. CeO_2 is used in various applications, such as gas sensors, catalysts, polishing materials, optical devices, sunscreen cosmetics, biotransformation, solid oxide fuel cells, etc. [28]. Among the metal nanoparticles, CeO_2 nanoparticles (CeO_2 NPs) have recently attracted

significant attention due to their unique surface chemistry, biocompatibility, and high stability [29]. In biological contexts, CeO_2 NPs have been reported to exhibit superoxide dismutase (SOD) and catalase (CAT) mimetic activities [30]. In addition, the biomedical and pharmacological properties of CeO_2 NPs have been demonstrated in many studies [31, 32]. Recently, nanoceria has also emerged as a promising nanocarrier for the delivery of diverse therapeutic molecules in cancer [33], wound healing [34], acute lung injury [35], etc. CeO_2 NPs can exert cytoprotective effects at physiological pH where these particles act as antioxidants; however, in an acidic environment like cancer cells, they are cytotoxic and act as prooxidants [36]. Meanwhile, several in vitro studies have reported the anti-cancer activity of the CeO_2 NPs on different cancer cell lines [37, 38].

In the current study, we reported the green synthesis of CeO_2 NPs using F. vulgaris leaf extract for the first time, and we evaluated their anti-cancer effects against PC3 human prostate cancer cells.

2. Materials and methods

2.1. Materials

Aerial parts of *F. vulgaris* were achieved from Kermanshah province (Iran) in spring. Ce(NO3)3.6H2O was purchased from Merck (Germany). RPMI 1640 cell culture media, phosphate buffered saline (PBS), penicillin plus streptomycin (pen/strep), fetal bovine serum (FBS), trypsin, and dimethyl sulfoxide (DMSO) were obtained from Sigma-Aldrich (St. Louis, MO, USA). Human low-differentiated prostate cancer cell line PC3 was purchased from Pasteur Institute of Iran (Tehran, Iran).

2.2. Preparation of *F. vulgaris* leaf extract

F. vulgaris leaves were washed with distilled water to remove dust and dirt, then 10.0 g of washed leaves were added to 100 ml of distilled water. This blend was stirred at 80 °C for 2 h; after that, the mixture was filtered, and leaf extract was stored at 4 °C for the subsequent steps.

2.3. Green synthesis of Cerium oxide nanoparticles

To synthesize CeO_2 NPs, 5.0 g of cerium nitrate dissolved in 20 ml water was added dropwise to 70 ml aqueous solution containing 10 ml of prepared *F. vulgaris* leaf extract and 60 ml distilled water. This solution was heated up to 80 °C and stirred continuously using a magnetic stirrer for 6 h. Afterward, the water was evaporated in an oven at 60 °C to achieve the gel. Finally, the obtained gel was calcinated at 400 °C in a furnace for 2 h to remove organic compounds [28, 39] and produce yellow powders of CeO_2 NPs [40].

2.4. Characterization

2.4.1. UV–visible spectroscopic characterization of CeO_2 NPs

The spectroscopic analysis of cerium oxide nanoparticles synthesized using *F. vulgaris* leaf extract was performed using a Cecil CE9500 UV-Vis spectrophotometer in the range of 200–650 nm.

2.4.2. X-ray diffraction (XRD) analysis

The X-ray diffraction patterns of the phyto-synthesized CeO_2 NPs were recorded on a D8-Advance Bruker X-ray diffractometer using Cu Kα1 radiation (λ=0.15406 nm).

2.4.3. Field-emission scanning electron microscopy (FESEM)

Morphological studies of the synthesized CeO_2 NPs were conducted by a field-emission scanning electron microscope (FESEM, TESCAN BRNO-Mira3 LMU).

2.4.4. Fourier transform infrared spectroscopy analysis

Fourier-transform infrared (FT-IR, Shimadzu 8400, Japan) measurements were performed in the spectral range of 400–4000 cm^{-1} to identify the functional groups present in the synthesized CeO_2 NPs.

2.4.5. Energy-dispersive X-ray spectroscopy (EDX) analysis of cerium oxide nanoparticles

Energy-dispersive X-ray (EDX) analysis was conducted to determine the elemental composition of the samples.

2.4.6. Transmission electron microscope analysis

The transmission electron microscopy (TEM, Philips Holland Tecnai-20) technique was used to distinguish the shape and size of the CeO_2 NPs.

2.5. Cell culture

The PC3 prostate cancer cells were cultured in RPMI 1640 medium enriched with 10% FBS, 2 mM glutamine, and 1% penicillin/streptomycin (100 µg/mL streptomycin and 100 U/mL penicillin) at 37 °C in a humidified atmosphere with 5% CO2.

2.6. Cytotoxicity assay

The Resazurin test, also known as the Alamar Blue assay, was used to evaluate the cytotoxic effects of biosynthesized CeO_2 NPs on the PC3 cancer cells. Resazurin is a soluble and non-fluorescent probe dye that can be metabolized to the strongly fluorescent resorufin by oxidoreductases within viable cells [41]. Briefly, a 100 µL culture medium containing 2×104 PC3 cells was seeded in 96-well plates and incubated for 24 h. Then, the cells were treated with different concentrations of biosynthesized CeO_2 NPs (3.9, 7.81, 15.62, 31.25, 62.5, 125, 250, and 500 µg/mL) [42] for 24 h at 37 °C in a humidified incubator with 5.0% CO_2. After that, the medium containing NPs was removed, and the cells were washed three times with PBS. Subsequently, 5.0 µL of Resazurin solution was added to each well and incubated in culture

condition for an additional 4 h. The fluorescence intensity was measured at 600 nm excitation and 570 nm emission wavelengths using a microplate fluorimeter (Perkin-Elmer). The IC_{50} value was determined using the GraphPad Prism® 6 software.

2.7. Quantitative real-time PCR (qRT-PCR) analysis for cell cycle, metastasis, and apoptotic markers

Human prostate cancer PC3 cells were cultured in 6-well plates and exposed to IC_{50} and 1/2 IC50 concentrations of photosynthesized CeO_2 NPs for 24 h. According to the manufacturer's instructions, total RNA was extracted using an RNA isolation kit at the end of exposure time (Yekta Tajhiz, Iran). The concentration and purity of total RNAs were measured by a Nanodrop spectrophotometer (NanoDrop 1000™, USA). Then, cDNA synthesis was done according to the Revert Aid First Strand cDNA Synthesis Kit (Parstous, Mashhad, Iran). Quantitative RT-PCR was performed in a commercial real-time thermocycler (Roche, Mannheim, Germany) with SYBR Green PCR Master Mix (Ampliqon, Denmark) according to the manufacturer's protocol. The glyceraldehyde-3-phosphate dehydrogenase (GAPDH) gene was also used as an internal reference gene. Finally, the relative quantifications of cyclin D1, C-myc, p21, Bax, B-cl-2, MMP-2, and MMP-9 mRNA to endogenous control housekeeping gene (GAPDH) mRNA expression levels were done (or calculated) by the formula $2^{-\Delta\Delta CT}$.

3. Results and discussion

CeO_2 NPs were successfully synthesized using *F. vulgaris* leaf extract through a simple green route in the present work. The results obtained from UV- visible, XRD, TEM, FESEM, EDX, and FTIR analysis demonstrated the nano-scale nature of biosynthesized NPs. *The in vitro* anti-cancer effects of the nanoparticles were also evaluated.

3.1. UV-visible spectroscopic analysis

The formation of CeO_2 NPs from *F. vulgaris* leaf extracts was initially confirmed by UV-vis absorption spectroscopy within the range of 200–650 nm. UV-Visible spectroscopy is one of the fundamental characterization tools to determine the optical properties of the nanoparticles [43]. The UV–Visible absorption spectrum of the biosynthesized CeO_2 NPs is given in Fig. 1A. The maximum absorption peak of CeO_2 NPs was observed at about 310 nm, which could be associated with the charge transfer transition from O2P to Ce4f [44]. Maqbool *et al*. [45] and Miri *et al*. [46] reported similar UV–Vis spectra for CeO_2 NPs synthesized using Olea europaea leaf and Ziziphus jujube fruit extract, respectively. In addition, the optical band gap of the CeO_2 NPs was estimated to be 3 eV from the UV-visible spectral results using the Tauc equation [47] (Fig. 1B).

3.2. X-ray diffraction analysis of synthesized CeO_2 NPs

The X-ray diffraction (XRD) technique was used to confirm the crystalline nature of the nanoparticles. The powder XRD patterns of the CeO_2 nanoparticles synthesized in *F. vulgaris* aqueous leaves extract is shown in figure 2. The XRD pattern indicated (111), (200), (220), (311), (222), (400), (331), (420) and (422) crystallographic planes depended to CeO_2. XRD data confirmed the crystallization of CeO_2 in a face-centered fluorite cubic system with Fm3m space group in accordance with the standard JCPDS card no. 34-0394 [48, 49]. No other characteristic peaks were observed in the pattern, indicating that the bio-synthesized CeO_2 NPs are pure after being calcined at 400 $^{\circ}$C. The Crystallite size of the prepared CeO_2 NPs was calculated using Debye–Scherrer's formula [50], and the average crystallite size of the sample was approximately 19.5 nm estimated.

3.3. FE-SEM analysis of CeO_2 NPs

Field Emission Scanning Electron Microscopy (FESEM) analysis was employed to determine the nanoparticles' surface morphology. The electron microscopical images of prepared CeO_2 nanoparticles were illustrated in figure 3 (A and B). From these images, it can be concluded that the particles are on a nanometer scale and are mostly spherical.

3.4. EDX pattern analysis of CeO_2 NPs

The chemical elemental analysis of green synthesized CeO_2 NPs was done using EDX. Figure 4shows the EDX spectrum of CeO_2 nanoparticles. The spectrum of EDX confirms the presence of Cerium and Oxygen in CeO_2 nanoparticles synthesized by using *F. vulgaris* leaf extracts.

3.5. FTIR studies

FT-IR spectroscopy measurements were performed to confirm the formation/ presence of the Ce-O band and to identify the functional groups in the leaf extract that may play a key role in the synthesis and stabilization of CeO_2 nanoparticles. FT-IR spectrum of green synthesized CeO_2 NPs is shown in Fig. 5. FT-IR spectra of CeO_2 NPs showed two characteristic absorption peaks at 463 cm^{-1} and 1111 cm^{-1} which may be related to Ce—O and O—Ce—O stretching bands, respectively, indicating the formation of CeO_2 NPs [51]. The spectral peak 3421 cm^{-1} could be assigned to the stretching vibration of the hydroxyl groups (–OH) and the physically adsorbed water on the surface of NPs [52, 53]. The presence of a peak at 1617 cm^{-1} is attributed to the stretching vibration of the C O functional group [54-56]. Moreover, other bands at 2897 cm^{-1}, 1471 cm^{-1}, and 1382 cm^{-1} may correspond to C–H stretching, bending, and rotating vibrations of residual organic compounds, respectively [57, 58].

3.6. TEM/PSA images

The TEM/PSA images of CeO_2 NPs are displayed in Fig. 6. (a, b), which were employed to investigate their shape, size, and distribution. TEM image displayed the spherical shape of biosynthesized CeO_2 NPs.

According to the PSA curve (Fig. 7b), the average size of nanoparticles was about 16 nm which conforms with the outcomes of the XRD pattern.

3.7. Cytotoxic Activity

The in vitro cytotoxic activity of biosynthesized CeO_2 NPs from the *F. vulgaris* leaf extract was tested at different concentrations (3.9, 7.81, 15.62, 31.25, 62.5, 125, 250, and 500 µg/mL) against PC3 human prostate cancer cells using the resazurin assay. As demonstrated in Fig. 7, a dose-dependent cytotoxic activity was observed in CeO_2 NPs-treated PC3 cells compared to the control cells. The half-maximal inhibitory concentration (IC_{50}) value of phytosynthesized CeO_2 NPs against PC3 cancer cells was about 113.6 µg/mL after 24 h treatment.

Similarly, several studies have also reported the concentration-dependent cytotoxic effects of CeO_2 NPs against A549 (human lung carcinoma) [59], MCF7 (breast cancer) [60], and HCT 116 (colorectal adenocarcinoma) [38] cell lines. Nanoceria can penetrate cancer cells through several endocytic pathways and exerts cytotoxic activity [61]. However, the toxicity mechanisms of CeO_2 NPs are not well understood. Meanwhile, it has been suggested that CeO_2 NPs can cause cell death via increasing ROS levels, cell cycle arrest, and activating apoptotic pathways [62, 63]. ROS typically contains the hydroxyl radical, superoxide radical, and hydrogen peroxide which can damage intracellular macromolecules (lipids, DNA, and proteins through oxidation and cause the cells to undergo apoptosis or necrosis. Nanoparticles can attach to the cancer cell surface and result in cell death by increasing intracellular ROS production [22]. Likewise, different biological resources that act as reducing and capping agents during the synthesis of NPs may influence the development of cytotoxicity [20, 64]. Many studies have recently indicated that the nanoparticles prepared using plant derivatives have a higher potential to control cancer cell growth [65, 66]. The improved cytotoxic effects can be due to the plant secondary metabolites involved in the green synthesis of NPs [67]. The current findings of the resazurin assay support the cytotoxic effect of green-synthesized CeO_2 NPs.

3.8. Real-time PCR

To further evaluate the anti-cancer potential of biosynthesized CeO_2 NPs on PC3 prostate cancer cells, the mRNA expression levels of cell cycle-related proteins (c-Myc, cyclin D1, p21), apoptosis-related genes (Bcl-2 and Bax), and migration-related genes (MMP-2 and MMP-9) were examined by real-time PCR.

As shown in Fig. 8, CeO_2 NPs, dose-dependently, reduced the expression levels of c-Myc, as an upstream of cell cycle-regulated genes, the anti-apoptotic gene (Bcl-2), and a G1-phase promoter (cyclin D1). Meanwhile, CeO_2 NPs increased the levels of the pro-apoptotic gene (Bax) and a negative regulator of the cell cycle (p21). Furthermore, CeO_2 NPs significantly reduced the expression levels of MMP-2 and MMP-9 in PC3 cells.

The MMP-2 (gelatinase A) and MMP-9 (gelatinase B) are two key members of the matrix metalloproteinase(MMPs) family. Overexpression of MMP-2 and MMP-9 have been reported in different human neoplasms, such as prostate cancer [68, 69]. There is accumulating evidence that the MMPs play an essential role in tumor cell invasion and metastasis by degrading the extracellular matrix (ECM) and membrane barriers [70]. Furthermore, MMPs can release various growth factors from ECM, which are directly involved in tumor angiogenesis [71]. Hence, blocking the expression of MMPs family can be a promising strategy for cancer therapy. In the present study, the CeO_2 NPs significantly reduced the mRNA expressions of MMP-2 and MMP-9 in the PC3 prostate cancer cells, suggesting that phytosynthesized CeO_2 NPs have a potent anti-metastatic effect on PC3 cells.

Apoptosis is a type of programmed cell death that can be triggered by various external and internal stimuli. The members of the Bcl-2 family, such as Bax and Bcl-2, have a pivotal role in regulating cellular life and death. The Bax has a pro-apoptotic effect, whereas the Bcl-2 is known for its anti-apoptotic activity [72]. In general, the induction of apoptosis is an attractive approach to cancer treatment. Therefore, many anti-tumor agents have been developed to induce the apoptotic process in cancer cells by targeting apoptosis-related genes [73, 74]. Meanwhile, several studies have suggested that metallic NPs can show anti-cancer activity against various cancer cells via increasing the expression of pro-apoptotic factors and reducing the expression of anti-apoptotic factors. The findings of a previous study revealed that phytosynthesized AgNPs possessed anti-cancer effects against PC-3 prostate cancer cells through elevating the expression level of Caspase-3 and remarkable reducing the expression levels of Bcl-2 and Survivin [22]. In this study, our data demonstrated that the phytosynthesized CeO2 NPs might induce an intrinsic signaling pathway for regulated cell death mediated by up-regulation of Bax and down-regulation of Bcl-2 gene expression on prostate cancer PC3 cells. Earlier studies have also shown that nanoceria stimulates apoptosis in other cancer cell lines through BAX/BCL2-dependent pathway [75]. However, further investigations are required to provide insight into the possible mechanisms involved in the anti-cancer activities of biosynthesized CeO2 NPs.

It is well known that cell cycle progression is closely related to tumorigenesis [76]. Meanwhile, many anti-cancer agents exert their growth inhibitory effects by inducing cell cycle arrest in tumor cells. The c-Myc is a key element in regulating diverse cellular functions such as cell growth, metabolism, differentiation, transformation, and apoptosis [77]. c-Myc promotes G1/S-phase cell cycle transition by increasing the expression of cyclins (A, E, D1, D2) and activating cyclin-dependent kinases (CDKs) [78]. Studies have indicated that the elevated c-Myc expression in human cancer cell lines can be associated with high proliferation rates and insensitivity to apoptotic stimuli [79]. Cyclin D1 is an essential cell cycle regulator, which plays a central role in cancer pathogenesis. It has been demonstrated that the overexpression of cyclin D1 may lead to uncontrolled cell cycle progression and malignant transformation [80]. Our results revealed that the biosynthesized CeO2 NPs could down-regulate mRNA expression of c-Myc and cyclin D1 in PC3 cells. These findings suggest that CeO2 NPs can inhibit cell growth in human prostate cancer cells by inducing cell cycle arrest.

4. Conclusion

In the present research, cerium oxide nanoparticles (CeO_2 NPs) were obtained using the aqueous extract of *Falcaria vulgaris* (*F. vulgaris*) through a facile, low-cost, and eco-friendly green route. The formation of phytosynthesized CeO_2 NPs was confirmed by various techniques, including UV–Vis, FE-SEM, EDX, TEM, XRD, and FT-IR Spectroscopy. The results showed that the CeO_2 NPs had a spherical shape with uniform and porous morphology. Moreover, the cell viability assay and real-time PCR tests were performed to evaluate the efficiency of biosynthesized CeO_2 NPs on the human prostate cancer cell lines PC3. The prepared nanoceria exhibited a significant anti-proliferative effect on the PC3 cancer cells in a dose-dependent manner. Additionally, our results demonstrated that the biosynthesized CeO_2 NPs could suppress cell metastasis, and promote cell cycle arrest as well as apoptosis in prostate cancer cells. Collectively, these findings suggest that the CeO_2 nanoparticles green-mediated by *F. vulgaris* extract can be used or considered as novel anti-cancer agents in the treatment of human prostate cancer.

Declarations

Ethical Approval: Not applicable

Competing interests: There is nothing to declare.

Authors' contributions: “D.T and H.A designed the experiments; H.A and S.E performed experiments and collected data; All authors discussed the results and strategy; S.I.H Supervised, directed and managed the study; D.T wrote the first draft of the paper, and all authors approved of the version to be published”.

Funding: There is nothing to declare.

Availability of data and materials: Original data are available upon a reasonable request.

References

1. Jahagirdar, A., et al., *Structural, EPR, optical and magnetic properties of α-Fe2O3 nanoparticles.* Spectrochimica Acta Part A: Molecular and Biomolecular Spectroscopy, 2013. **104**: p. 512-518.
2. Sajid, M. and J. Płotka-Wasylka, *Nanoparticles: Synthesis, characteristics, and applications in analytical and other sciences.* Microchemical Journal, 2020. **154**: p. 104623.
3. Diallo, A., et al., *Luminescent Eu2O3 nanocrystals by Aspalathus linearis' extract: structural and optical properties.* Journal of nanophotonics, 2016. **10**(2): p. 026010.
4. Jamdagni, P., P. Khatri, and J. Rana, *Nanoparticles based DNA conjugates for detection of pathogenic microorganisms.* International Nano Letters, 2016. **6**(3): p. 139-146.
5. Singh, R.P., R. Handa, and G. Manchanda, *Nanoparticles in sustainable agriculture: An emerging opportunity.* Journal of Controlled Release, 2020.

6. You, J., et al., *Metal oxide nanoparticles as an electron-transport layer in high-performance and stable inverted polymer solar cells.* Advanced Materials, 2012. **24**(38): p. 5267-5272.
7. Liu, X., et al., *Noble metal–metal oxide nanohybrids with tailored nanostructures for efficient solar energy conversion, photocatalysis and environmental remediation.* Energy & Environmental Science, 2017. **10**(2): p. 402-434.
8. McNamara, K. and S.A. Tofail, *Nanoparticles in biomedical applications.* Advances in Physics: X, 2017. **2**(1): p. 54-88.
9. Singh, N., et al., *NanoGenotoxicology: the DNA damaging potential of engineered nanomaterials.* Biomaterials, 2009. **30**(23-24): p. 3891-3914.
10. Kwon, J.Y., P. Koedrith, and Y.R. Seo, *Current investigations into the genotoxicity of zinc oxide and silica nanoparticles in mammalian models in vitro and in vivo: carcinogenic/genotoxic potential, relevant mechanisms and biomarkers, artifacts, and limitations.* International Journal of Nanomedicine, 2014. **9**(Suppl 2): p. 271.
11. Sabir, S., M. Arshad, and S.K. Chaudhari, *Zinc oxide nanoparticles for revolutionizing agriculture: synthesis and applications.* The Scientific World Journal, 2014. **2014**.
12. Luque, P., et al., *Green synthesis of zinc oxide nanoparticles using Citrus sinensis extract.* Journal of Materials Science: Materials in Electronics, 2018. **29**(12): p. 9764-9770.
13. Saravanan, M., et al., *Emerging theranostic silver and gold nanobiomaterials for breast cancer: Present status and future prospects*, in *Handbook on Nanobiomaterials for Therapeutics and Diagnostic Applications*. 2021, Elsevier. p. 439-456.
14. Saravanan, M., et al., *Emerging antineoplastic biogenic gold nanomaterials for breast cancer therapeutics: a systematic review.* International Journal of Nanomedicine, 2020. **15**: p. 3577.
15. Hussain, I., et al., *Green synthesis of nanoparticles and its potential application.* Biotechnology letters, 2016. **38**(4): p. 545-560.
16. Jadoun, S., et al., *Green synthesis of nanoparticles using plant extracts: A review.* Environmental Chemistry Letters, 2021. **19**(1): p. 355-374.
17. Makarov, V., et al., *"Green" nanotechnologies: synthesis of metal nanoparticles using plants.* Acta Naturae (англоязычная версия), 2014. **6**(1 (20)).
18. Barabadi, H., et al., *Green nanotechnology-based gold nanomaterials for hepatic cancer therapeutics: a systematic review.* Iranian Journal of Pharmaceutical Research: IJPR, 2020. **19**(3): p. 3.
19. Barabadi, H., et al., *Emerging theranostic silver nanomaterials to combat lung cancer: a systematic review.* Journal of Cluster Science, 2020. **31**(1): p. 1-10.
20. Barabadi, H., et al., *Emerging antineoplastic gold nanomaterials for cervical cancer therapeutics: a systematic review.* Journal of Cluster Science, 2020. **31**(6): p. 1173-1184.
21. Barabadi, H., et al., *Antineoplastic biogenic silver nanomaterials to combat cervical cancer: a novel approach in cancer therapeutics.* Journal of Cluster Science, 2020. **31**(4): p. 659-672.

22. Barabadi, H., et al., *Emerging theranostic silver and gold nanomaterials to combat prostate cancer: a systematic review.* Journal of Cluster Science, 2019. **30**(6): p. 1375-1382.
23. Jalili, C., S. Roshankhah, and M.R. Salahshoor, *Falcaria vulgaris extract attenuates ethanol-induced renal damage by reducing oxidative stress and lipid peroxidation in rats.* Journal of pharmacy & bioallied sciences, 2019. **11**(3): p. 268.
24. Zangeneh, M.M., *Green synthesis and chemical characterization of silver nanoparticles from aqueous extract of Falcaria vulgaris leaves and assessment of their cytotoxicity and antioxidant, antibacterial, antifungal and cutaneous wound healing properties.* Applied Organometallic Chemistry, 2019. **33**(9): p. e4963.
25. Goorani, S., et al., *Assessment of antioxidant and cutaneous wound healing effects of Falcaria vulgaris aqueous extract in Wistar male rats.* Comparative Clinical Pathology, 2019. **28**(2): p. 435-445.
26. Zangeneh, M.M., et al., *Preparation, characterization, and evaluation of cytotoxicity, antioxidant, cutaneous wound healing, antibacterial, and antifungal effects of gold nanoparticles using the aqueous extract of Falcaria vulgaris leaves.* Applied Organometallic Chemistry, 2019. **33**(11): p. e5216.
27. Charbgoo, F., M.B. Ahmad, and M. Darroudi, *Cerium oxide nanoparticles: green synthesis and biological applications.* International journal of nanomedicine, 2017. **12**: p. 1401.
28. Arumugam, A., et al., *Synthesis of cerium oxide nanoparticles using Gloriosa superba L. leaf extract and their structural, optical and antibacterial properties.* Materials Science and Engineering: C, 2015. **49**: p. 408-415.
29. Rajeshkumar, S. and P. Naik, *Synthesis and biomedical applications of cerium oxide nanoparticles–a review.* Biotechnology Reports, 2018. **17**: p. 1-5.
30. Singh, R. and S. Singh, *Role of phosphate on stability and catalase mimetic activity of cerium oxide nanoparticles.* Colloids and Surfaces B: Biointerfaces, 2015. **132**: p. 78-84.
31. Celardo, I., et al., *Pharmacological potential of cerium oxide nanoparticles.* Nanoscale, 2011. **3**(4): p. 1411-1420.
32. Wason, M.S. and J. Zhao, *Cerium oxide nanoparticles: potential applications for cancer and other diseases.* American journal of translational research, 2013. **5**(2): p. 126.
33. Sack, M., et al., *Combination of conventional chemotherapeutics with redox-active cerium oxide nanoparticles—a novel aspect in cancer therapy.* Molecular cancer therapeutics, 2014. **13**(7): p. 1740-1749.
34. Rather, H.A., et al., *Antioxidative study of Cerium Oxide nanoparticle functionalised PCL-Gelatin electrospun fibers for wound healing application.* Bioactive materials, 2018. **3**(2): p. 201-211.
35. Niemiec, S.M., et al., *Cerium oxide nanoparticle delivery of microRNA-146a for local treatment of acute lung injury.* Nanomedicine: Nanotechnology, Biology and Medicine, 2021. **34**: p. 102388.
36. Miri, A., M. Darroudi, and M. Sarani, *Biosynthesis of cerium oxide nanoparticles and its cytotoxicity survey against colon cancer cell line.* Applied Organometallic Chemistry, 2020. **34**(1): p. e5308.

37. Sridharan, M., et al., *Synthesis, characterization and evaluation of biosynthesized cerium oxide nanoparticle for its anticancer activity on breast cancer cell (mcf 7).* Materials Today: Proceedings, 2021. **36**: p. 914-919.
38. Datta, A., et al., *Pro-oxidant therapeutic activities of cerium oxide nanoparticles in colorectal carcinoma cells.* ACS omega, 2020. **5**(17): p. 9714-9723.
39. Elahi, B., et al., *Preparation of cerium oxide nanoparticles in Salvia Macrosiphon Boiss seeds extract and investigation of their photo-catalytic activities.* Ceramics International, 2019. **45**(4): p. 4790-4797.
40. Elahi, B., et al., *Bio-based synthesis of Nano-Ceria and evaluation of its bio-distribution and biological properties.* Colloids and Surfaces B: Biointerfaces, 2019. **181**: p. 830-836.
41. Javid, H., et al., *The role of substance P/neurokinin 1 receptor in the pathogenesis of esophageal squamous cell carcinoma through constitutively active PI3K/Akt/NF-κB signal transduction pathways.* Molecular biology reports, 2020. **47**(3): p. 2253-2263.
42. Nazaripour, E., et al., *Biosynthesis of lead oxide and cerium oxide nanoparticles and their cytotoxic activities against colon cancer cell line.* Inorganic Chemistry Communications, 2021. **131**: p. 108800.
43. Goharshadi, E.K., S. Samiee, and P. Nancarrow, *Fabrication of cerium oxide nanoparticles: Characterization and optical properties.* Journal of colloid and interface science, 2011. **356**(2): p. 473-480.
44. Ansari, A.A., et al., *Synthesis, structural and optical properties of Mn-doped ceria nanoparticles: a promising catalytic material.* Acta Metallurgica Sinica (English Letters), 2016. **29**(3): p. 265-273.
45. Maqbool, Q., et al., *Antimicrobial potential of green synthesized CeO2 nanoparticles from Olea europaea leaf extract.* International journal of nanomedicine, 2016. **11**: p. 5015.
46. Miri, A., S. Akbarpour Birjandi, and M. Sarani, *Survey of cytotoxic and UV protection effects of biosynthesized cerium oxide nanoparticles.* Journal of biochemical and molecular toxicology, 2020. **34**(6): p. e22475.
47. Li, S., et al., *Facile synthesis of cerium oxide nanoparticles decorated flower-like bismuth molybdate for enhanced photocatalytic activity toward organic pollutant degradation.* Journal of colloid and interface science, 2018. **530**: p. 171-178.
48. Hancock, M.L., et al., *The characterization of purified citrate-coated cerium oxide nanoparticles prepared via hydrothermal synthesis.* Applied Surface Science, 2021. **535**: p. 147681.
49. Kouser, S., et al., *Sunlight-assisted synthesis of cerium (IV) oxide nanostructure with enhanced photocatalytic activity.* Optik, 2021. **245**: p. 167236.
50. Patterson, A., *The Scherrer formula for X-ray particle size determination.* Physical review, 1939. **56**(10): p. 978.
51. Sreekanth, T., G. Dillip, and Y.R. Lee, *Picrasma quassioides mediated cerium oxide nanostructures and their post-annealing treatment on the microstructural, morphological and enhanced catalytic performance.* Ceramics International, 2016. **42**(6): p. 6610-6618.

52. Ramjeyanthi, N., M. Alagar, and D. Muthuraman, *Synthesis, structural and optical behavior of cerium oxide nanoparticles by co-precipitation method.* Int. J. Sci. Res. Sci. Technol., 2018. **4**: p. 1009-1013.
53. Ahmed, H.E., et al., *Green Synthesis of CeO2 Nanoparticles from the Abelmoschus esculentus Extract: Evaluation of Antioxidant, Anticancer, Antibacterial, and Wound-Healing Activities.* Molecules, 2021. **26**(15): p. 4659.
54. Sulaiman, G.M., A.T. Tawfeeq, and A.S. Naji, *Biosynthesis, characterization of magnetic iron oxide nanoparticles and evaluations of the cytotoxicity and DNA damage of human breast carcinoma cell lines.* Artificial cells, nanomedicine, and biotechnology, 2018. **46**(6): p. 1215-1229.
55. Ismail, M., et al., *Green synthesis of zerovalent copper nanoparticles for efficient reduction of toxic azo dyes congo red and methyl orange.* Green processing and synthesis, 2019. **8**(1): p. 135-143.
56. Erjaee, H., H. Rajaian, and S. Nazifi, *Synthesis and characterization of novel silver nanoparticles using Chamaemelum nobile extract for antibacterial application.* Advances in Natural Sciences: Nanoscience and Nanotechnology, 2017. **8**(2): p. 025004.
57. Awwad, A.M., N.M. Salem, and A.O. Abdeen, *Green synthesis of silver nanoparticles using carob leaf extract and its antibacterial activity.* International journal of Industrial chemistry, 2013. **4**(1): p. 1-6.
58. Santhoshkumar, J., et al., *A biological synthesis of copper nanoparticles and its potential applications*, in *Green Synthesis, Characterization and Applications of Nanoparticles*. 2019, Elsevier. p. 199-221.
59. Lin, W., et al., *Toxicity of cerium oxide nanoparticles in human lung cancer cells.* International journal of toxicology, 2006. **25**(6): p. 451-457.
60. Javadi, F., et al., *Biosynthesis, characterization of cerium oxide nanoparticles using Ceratonia siliqua and evaluation of antioxidant and cytotoxicity activities.* Materials Research Express, 2019. **6**(6): p. 065408.
61. Chen, B.-H. and B. Stephen Inbaraj, *Various physicochemical and surface properties controlling the bioactivity of cerium oxide nanoparticles.* Critical reviews in biotechnology, 2018. **38**(7): p. 1003-1024.
62. Wason, M.S., et al., *Cerium oxide nanoparticles sensitize pancreatic cancer to radiation therapy through oxidative activation of the JNK apoptotic pathway.* Cancers, 2018. **10**(9): p. 303.
63. Nourmohammadi, E., et al., *Cerium oxide nanoparticles: A promising tool for the treatment of fibrosarcoma in-vivo.* Materials Science and Engineering: C, 2020. **109**: p. 110533.
64. Barabadi, H., et al., *Emerging theranostic gold nanomaterials to combat lung cancer: a systematic review.* Journal of Cluster Science, 2020. **31**(2): p. 323-330.
65. Mousavi, B., F. Tafvizi, and S. Zaker Bostanabad, *Green synthesis of silver nanoparticles using Artemisia turcomanica leaf extract and the study of anti-cancer effect and apoptosis induction on gastric cancer cell line (AGS).* Artificial cells, nanomedicine, and biotechnology, 2018. **46**(sup1): p. 499-510.
66. Kuppusamy, P., et al., *Biosynthesis of metallic nanoparticles using plant derivatives and their new avenues in pharmacological applications–An updated report.* Saudi Pharmaceutical Journal, 2016.

24(4): p. 473-484.

67. Padalia, H. and S. Chanda, *Characterization, antifungal and cytotoxic evaluation of green synthesized zinc oxide nanoparticles using Ziziphus nummularia leaf extract.* Artificial cells, nanomedicine, and biotechnology, 2017. **45**(8): p. 1751-1761.
68. Xiao, L.-J., et al., *ADAM17 targets MMP-2 and MMP-9 via EGFR-MEK-ERK pathway activation to promote prostate cancer cell invasion.* International journal of oncology, 2012. **40**(5): p. 1714-1724.
69. Mehta, P., et al., *MEK5 overexpression is associated with metastatic prostate cancer, and stimulates proliferation, MMP-9 expression and invasion.* Oncogene, 2003. **22**(9): p. 1381-1389.
70. Egeblad, M. and Z. Werb, *New functions for the matrix metalloproteinases in cancer progression.* Nature reviews cancer, 2002. **2**(3): p. 161-174.
71. Fink, K. and J. Boratyński, *The role of metalloproteinases in modification of extracellular matrix in invasive tumor growth, metastasis and angiogenesis.* Postepy higieny i medycyny doswiadczalnej (Online), 2012. **66**: p. 609-628.
72. Ola, M.S., M. Nawaz, and H. Ahsan, *Role of Bcl-2 family proteins and caspases in the regulation of apoptosis.* Molecular and cellular biochemistry, 2011. **351**(1): p. 41-58.
73. Katifelis, H., et al., *Ag/Au bimetallic nanoparticles induce apoptosis in human cancer cell lines via P53, CASPASE-3 and BAX/BCL-2 pathways.* Artificial cells, nanomedicine, and biotechnology, 2018. **46**(sup3): p. S389-S398.
74. Amiri, H., et al., *Green synthesized selenium nanoparticles for ovarian cancer cell apoptosis.* Research on Chemical Intermediates, 2021. **47**(6): p. 2539-2556.
75. Nourmohammadi, E., et al., *Evaluation of anticancer effects of cerium oxide nanoparticles on mouse fibrosarcoma cell line.* Journal of cellular physiology, 2019. **234**(4): p. 4987-4996.
76. Dang, F., L. Nie, and W. Wei, *Ubiquitin signaling in cell cycle control and tumorigenesis.* Cell Death & Differentiation, 2021. **28**(2): p. 427-438.
77. Yao, R., et al., *Identification of a Novel c-Myc Inhibitor 7594-0037 by Structure-Based Virtual Screening and Investigation of Its Anti-Cancer Effect on Multiple Myeloma.* Drug Design, Development and Therapy, 2020. **14**: p. 3983.
78. Faouzi, M., et al., *ORAI3 silencing alters cell proliferation and cell cycle progression via c-myc pathway in breast cancer cells.* Biochimica et Biophysica Acta (BBA)-Molecular Cell Research, 2013. **1833**(3): p. 752-760.
79. Zhou, L., et al., *Theabrownin inhibits cell cycle progression and tumor growth of lung carcinoma through c-myc-related mechanism.* Frontiers in pharmacology, 2017. **8**: p. 75.
80. Montalto, F.I. and F. De Amicis, *Cyclin D1 in cancer: a molecular connection for cell cycle control, adhesion and invasion in tumor and stroma.* Cells, 2020. **9**(12): p. 2648.

Figures

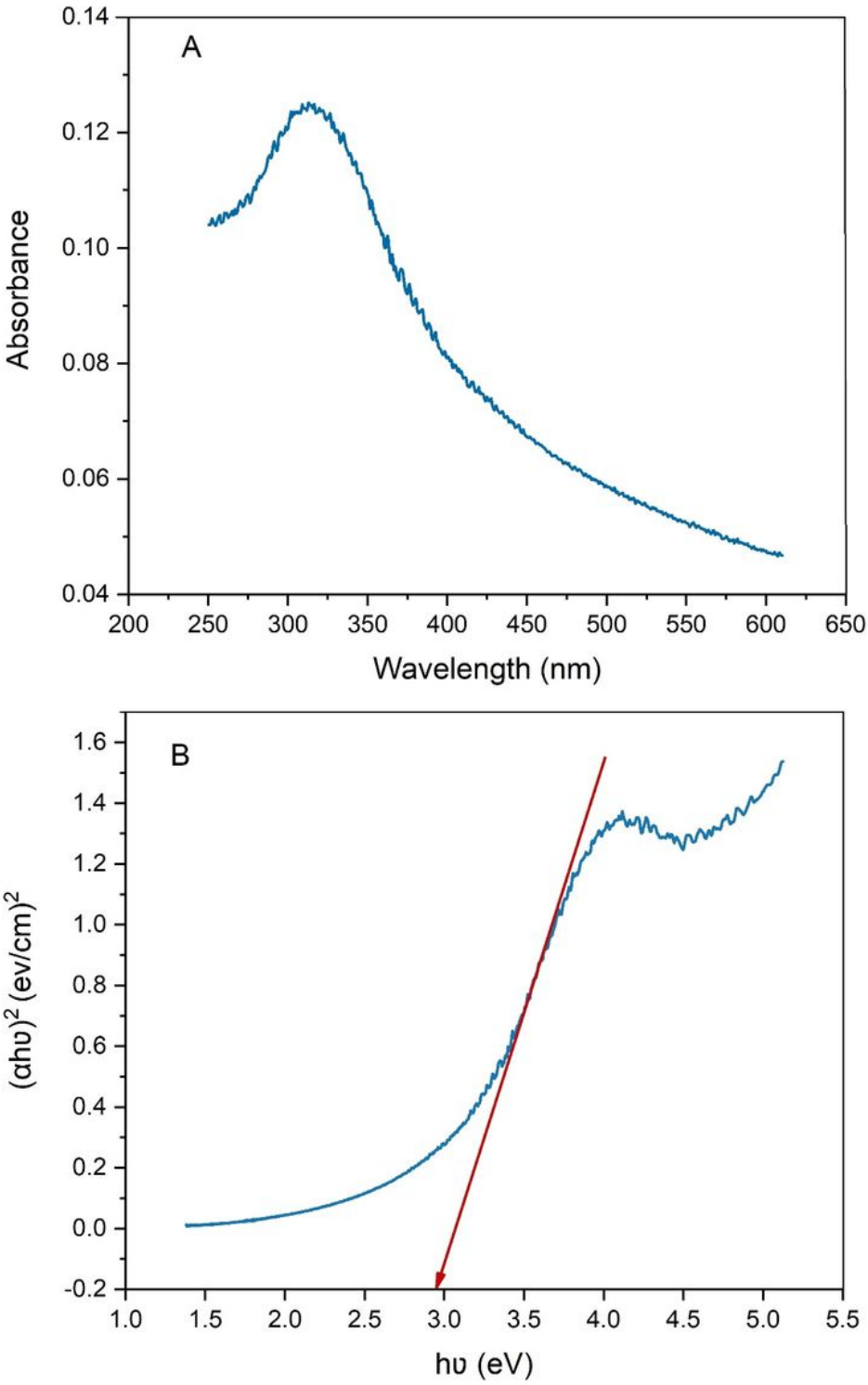


Figure 1

UV-Vis spectrum with a maximum absorption peak at about 310 nm (A) and band gap energy (B) of CeO_2 NPs synthesized using *F. vulgaris* leaf extract.

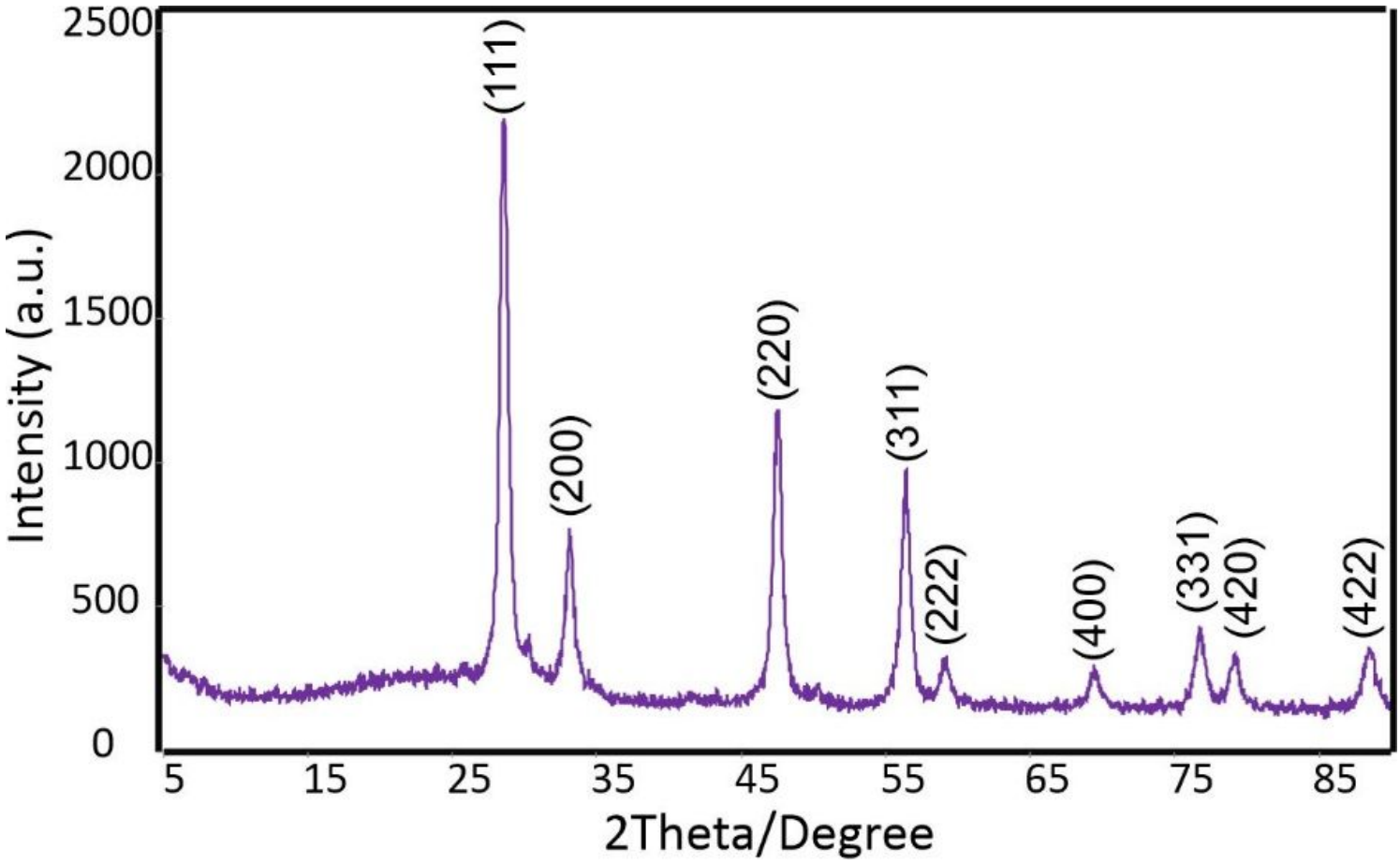


Figure 2

XRD spectrum of CeO_2 NPs synthesized using *F. vulgaris* leaf extract.

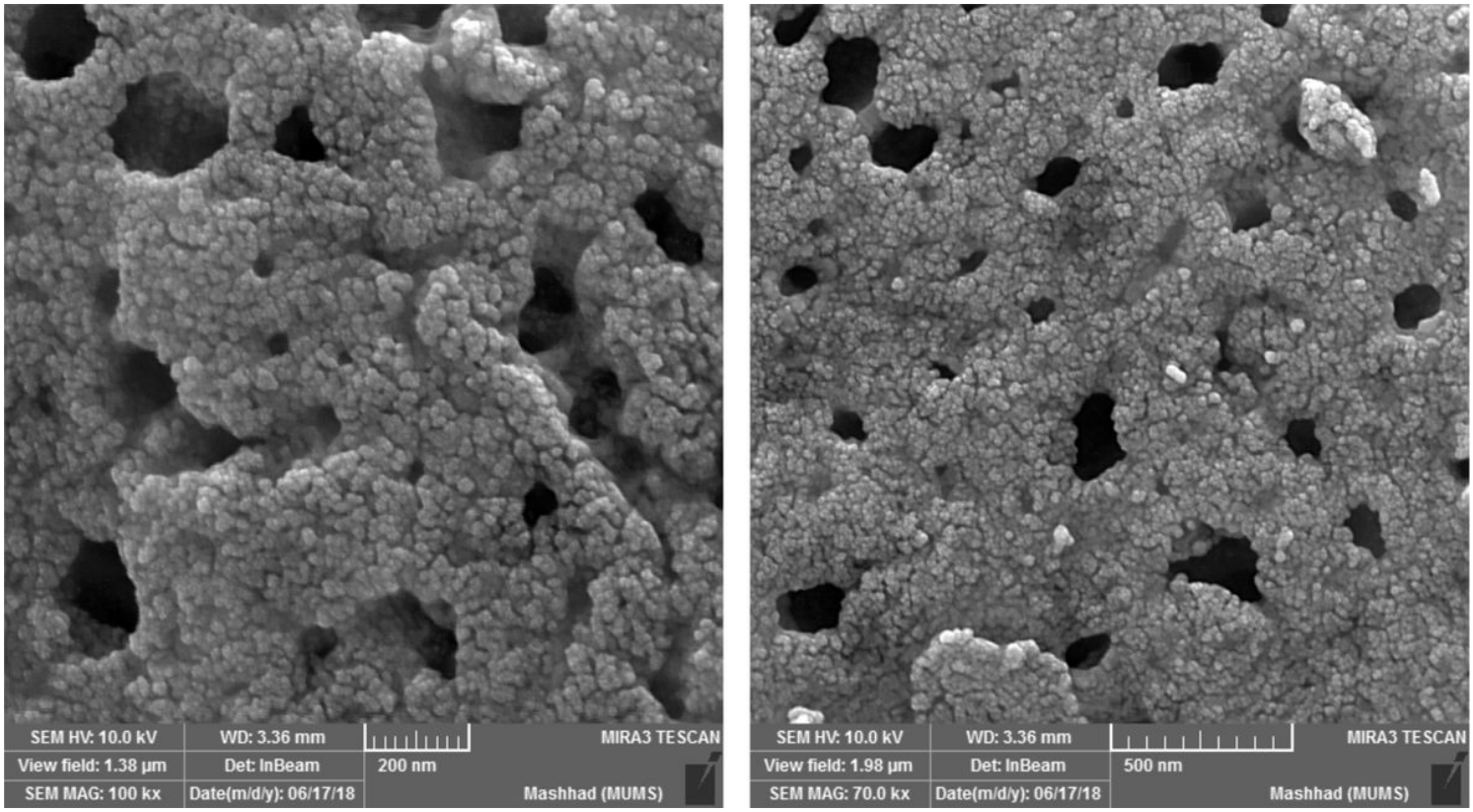


Figure 3

FE-SEM images of synthesized CeO_2 NPs.

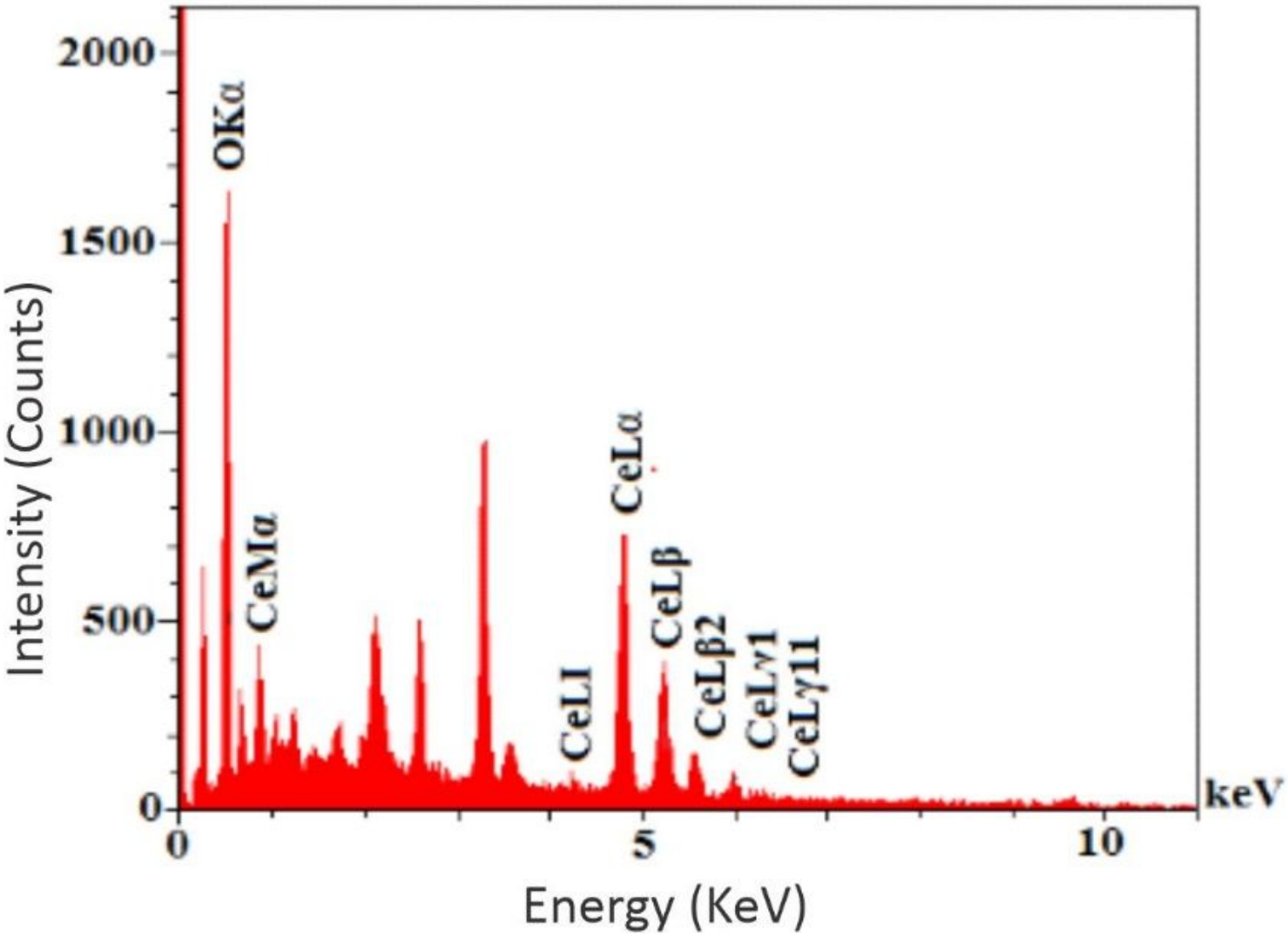


Figure 4

EDX Spectrum of synthesized CeO_2 NPs from leaf extract of *F. vulgaris*, showing the presence of Cerium and Oxygen in CeO_2 nanoparticles.

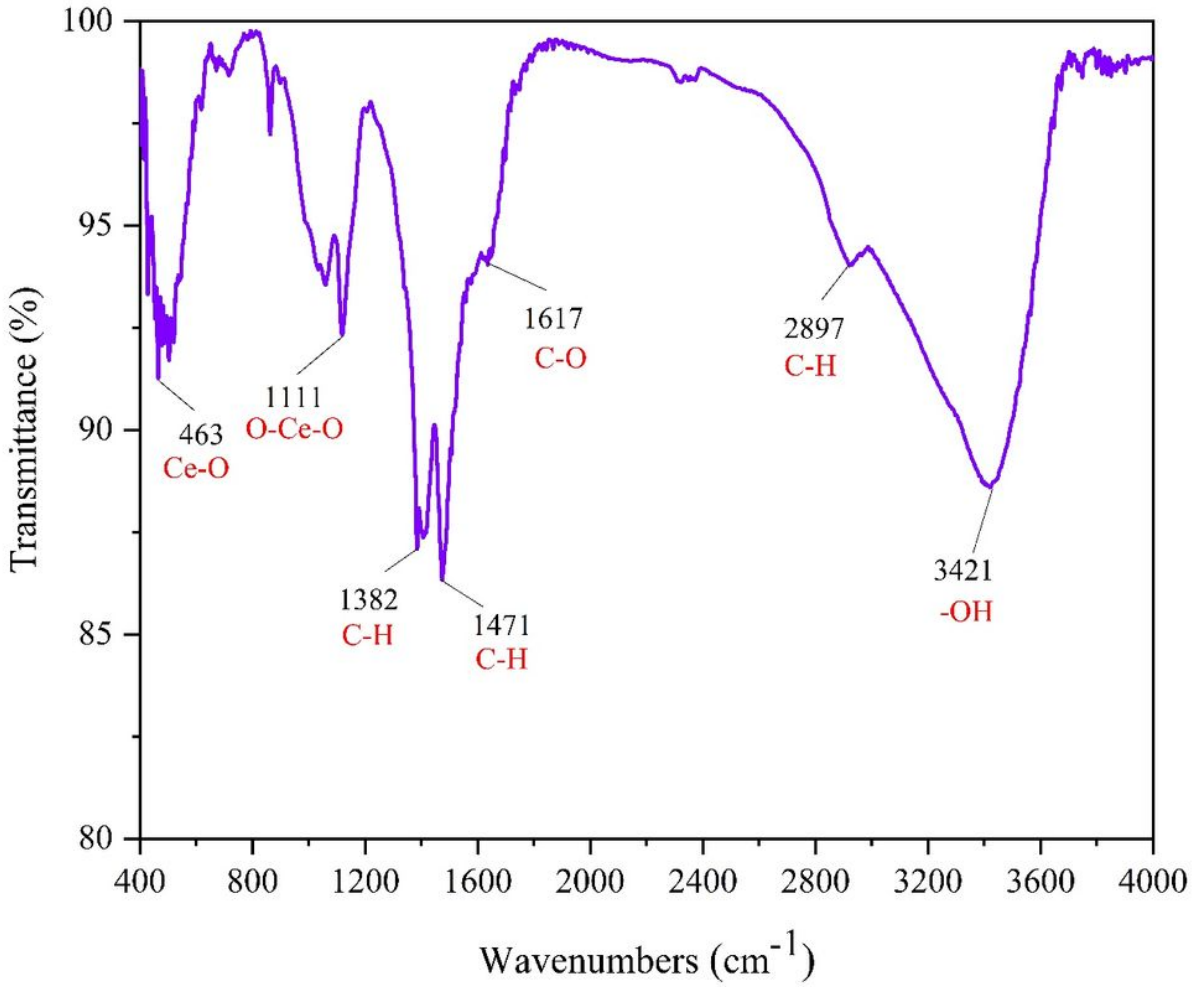


Figure 5

FT-IR spectrum of CeO_2 NPs synthesized by *F. vulgaris* leaf extract.

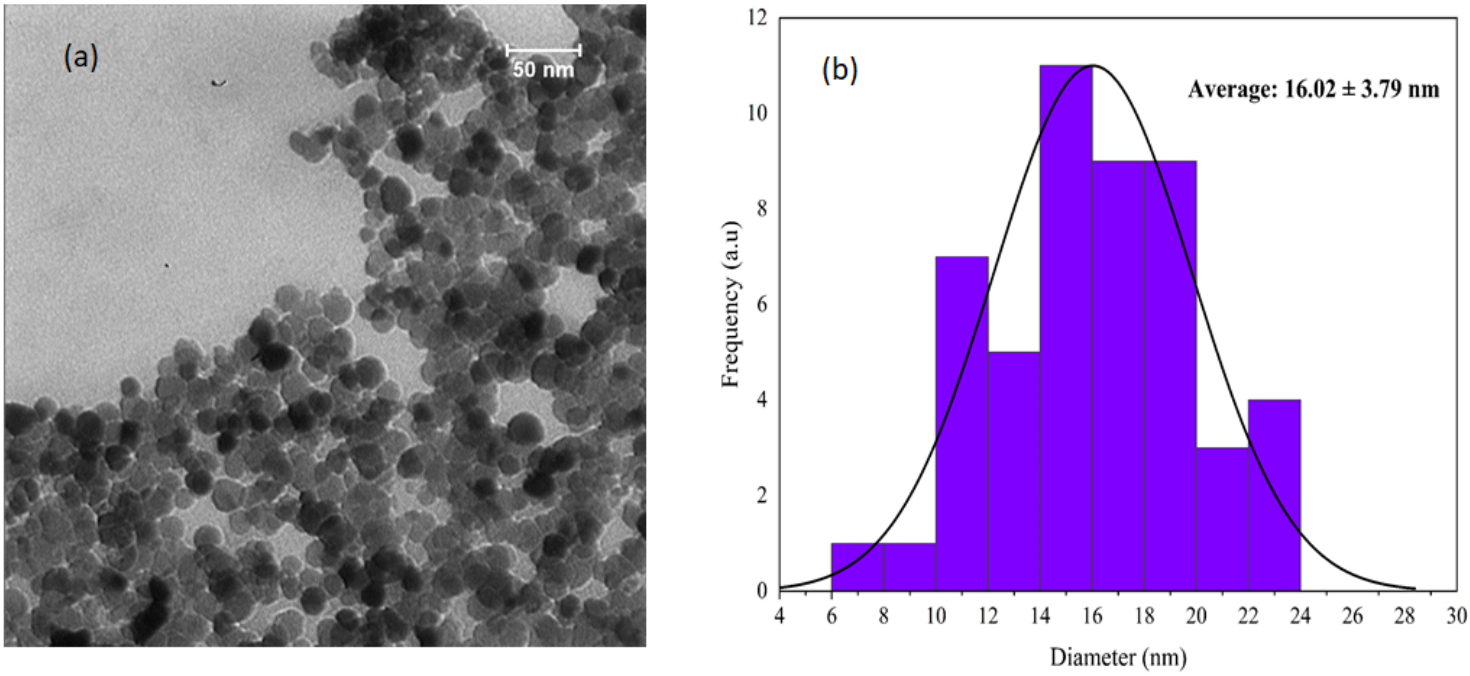


Figure 6

TEM micrograph (a) and particles size distribution (b) of CeO_2 NPs

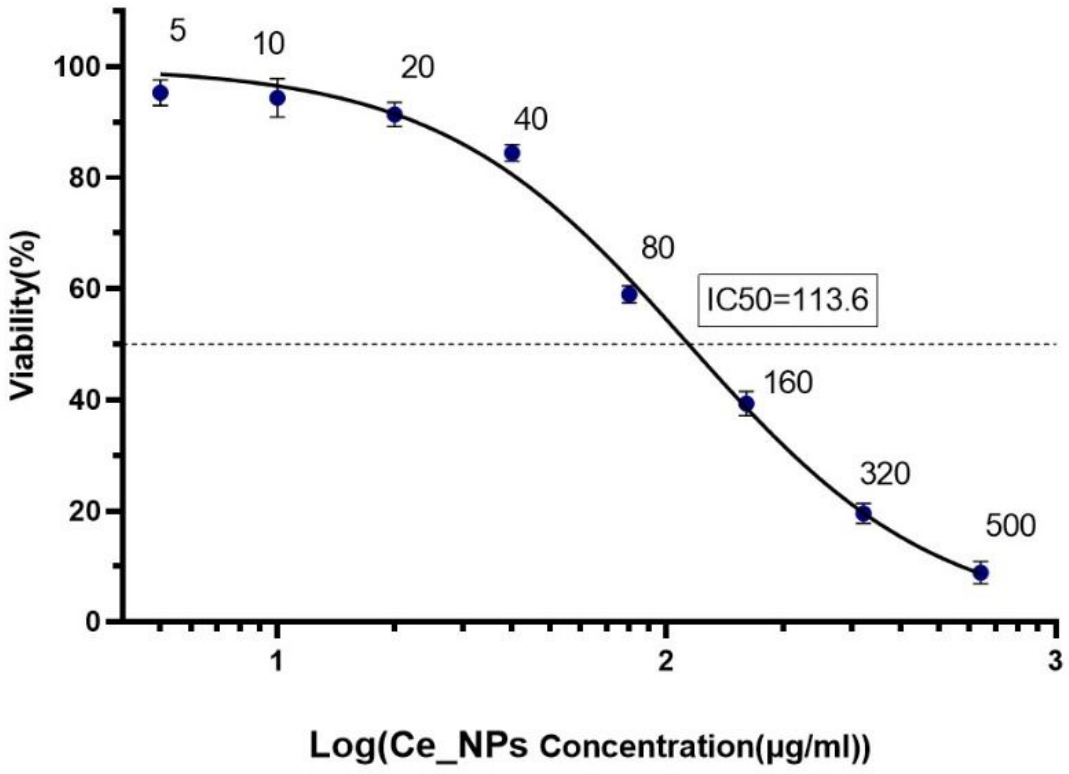


Figure 7

The cell viability of PC3 cancer cells after treating with the biosynthesized CeO_2 NPs for 24 h at the different concentrations by the resazurin assay.

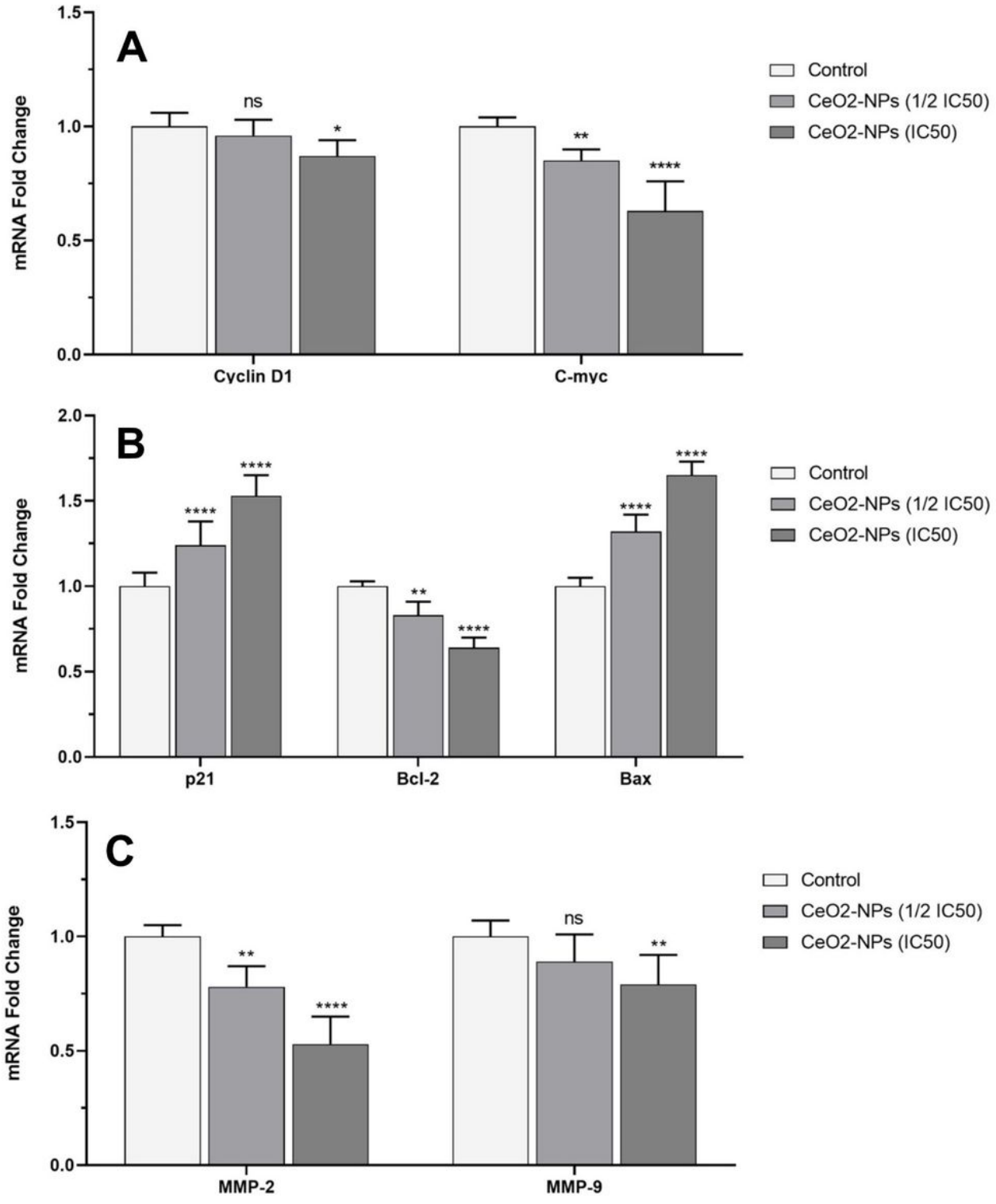


Figure 8

Prostate cancer cells (PC3) were treated with the biosynthesized CeO_2 NPs for 24 h with two different concentrations (IC50 and 1/2 IC50). After that, the mRNA expression levels of cell cycle-related proteins

(Cyclin D1 and c-Myc) (**A**), apoptosis-related genes (p21, Bcl-2, and Bax) (**B**), and migration-related genes (MMP-2 and MMP-9) (**C**) were assessed by qRT-PCR. The experiments were carried out in triplicates, and results are shown as the mean ± SD. Statistical significance was determined at (*P ≤ 0.05; **P ≤ 0.01; ***P ≤ 0.001; **** P ≤ 0.0001).